Yrast decay schemes from heavy-ion + ^{48}Ca fusion-evaporation reactions: IV: ^{53}Cr, ^{54}V, ^{62}Co, and $^{61-63}$Ni†

E. K. Warburton, J. W. Olness, A. M. Nathan,* and A. R. Poletti‡
Brookhaven National Laboratory, Upton, New York 11973
(Received 25 May 1978)

Fusion-evaporation reactions induced by beams of 25–55 MeV ^{9}Be and ^{18}O on an isotopically enriched ^{48}Ca target have been used to populate high-spin yrast levels in ^{53}Cr, ^{54}V, ^{62}Co, and $^{61-63}$Ni. Measurements consisted of γ-ray excitation functions, angular distributions, γ-γ coincidences, and recoil-distance and Doppler shift lifetime measurements, from which were deduced the energy levels, γ-ray branching ratios, most probable spin-parity assignments, and level lifetimes.

[NUCLEAR REACTIONS ^{48}Ca(^{9}Be, xn, yp)^{53}Cr and ^{54}V. ^{48}Ca(^{18}O, xn)$^{61-63}$Ni and ^{48}Ca(^{18}O, $3n,p$)^{62}Co. E=25–55 MeV; measured $\sigma(E,E_\gamma)$ and coin; deduced levels; measured $\sigma(E_\gamma,\theta)$; deduced J^π for high-spin levels; measured RDM and DSA; deduced τ_m, $|M(M1)|^2$ and $|M(E2)|^2$. Enriched targets, Ge(Li) detectors.]

I. INTRODUCTION

In this fourth in a series of reports of high-spin yrast decay schemes in nuclei formed by heavy-ion (HI) + ^{48}Ca fusion-evaporation reactions, we report on ^{53}Cr, ^{54}V, ^{62}Co, and $^{61-63}$Ni. These nuclei were formed by the reactions ^{48}Ca(^{9}Be, $4n$)^{53}Cr, ^{48}Ca(^{9}Be, $2np$)^{54}V, ^{48}Ca(^{18}O, $3np$)^{62}Co, ^{48}Ca(^{18}O, $5n$)^{61}Ni, ^{48}Ca(^{18}O, $4n$)^{62}Ni, and ^{48}Ca(^{18}O, $3n$)^{63}Ni.

In the first three reports in this series (hereafter referred to as I,[1] II,[2] and III[3]) we reported on results for nuclei in the range A = 54 to 60 formed via bombardment of ^{48}Ca by ^{11}B, ^{13}C, ^{15}N, and ^{18}O. This report is the last in the series and completes an investigation of the yrast levels in nuclei formed via the most intense exit channels in the bombardment of ^{48}Ca with ^{9}Be, ^{11}B, ^{13}C, ^{15}N, and ^{18}O projectiles at bombarding energies $\leq$60 MeV. Results for ^{6,7}Li + ^{48}Ca (and ^{6,7}Li + ^{51}V) have also been reported from this laboratory.[4]

The experimental investigations included γ-ray excitation functions and angular distributions, γ − γ coincidence spectra, and lifetime measurements via the Doppler-shift-attenuation method (DSAM) and recoil-distance method (RDM). These procedures, the data analysis methods, and criteria for establishing decay schemes and spin-parity assignments or preferences have been fully described in I, to which the reader is referred for a more complete discussion and presentation. In I, II, and III we described the systematic dependence of HI + ^{48}Ca fusion-evaporation products on bombarding energy for projectiles of ^{11}B, ^{13}C, ^{15}N, and ^{18}O. The yield curves for ^{9}Be + ^{48}Ca and ^{18}O + ^{48}Ca have the same general behavior as these others, as is expected since the compound nuclei for bombardment of ^{48}Ca via these projectiles all have nearly the same relative position *vis a vis* the valley of stability. Thus, at 45-MeV bombarding energy where most of the ^{18}O + ^{48}Ca measurements were made, ^{62}Ni was the most intense nucleus formed with ^{59}Fe, ^{61}Ni, ^{63}Ni, ^{62}Co, and ^{60}Fe following in that order. Results for $^{59-60}$Fe have already been reported.[2] The quality and quantity of the information obtained on these nuclei varies approximately as the intensity of formation. The formation of ^{63}Co with an intensity comparable to that of ^{60}Fe was expected from the local systematics.[1-4] However, no γ rays were observed which could be identified with ^{63}Co which has only been studied via the ^{64}Ni(t,α) reaction.[5] For ^{9}Be + ^{48}Ca, ^{50,51}Ti, and ^{53}V were also formed quite strongly at 27- and 35-MeV bombarding energy where the angular distributions and γ-γ coincidences, respectively, were taken, but in all three cases no information was obtained which was not available from other sources. However, the study did provide new information on ^{53}Cr and ^{54}V.

In the next section we present the decay schemes deduced from these data. In the final section we discuss specific aspects of the results with respect to the systematics revealed in the complete series of studies. A composite listing of the γ rays observed in the reactions HI + ^{48}Ca studied to date, prepared in a form similar to that presented in Table II of I, is available upon request to one of the authors (E. K. W.).

TABLE I. γ Decay of ^{53}Cr from ^{48}Ca(^{9}Be, $4n$) ^{53}Cr.

E_i [a] (keV)	E_f (keV)	E_γ [b] (keV)	Branching ratio (%)	Angular distribution [c] I_γ	A_2 (%)	A_4 (%)	$F(\tau)$ [d] (%)	Mean life [e] (ps)
1006.49(10)	0	1006.49(11)	100	107299	5(3)	6(3)	<0.20	~2.5 [f]
1289.62(10)	0	1289.59(11)	94(1)	290876	34(3)	−8(4)	0.08(2)	1.60(15) [f]
	1006	283.14(11)	6(1)	19187	−20(3)	0	<0.20	
1536.72(10)	0	1536.73(10)	9(2)	8146	31(6)	−6(6)	<0.30	33.3(1.1) [g]
	1006	530.18(11)	65(2)	60632	−18(2)	0	<0.40	
	1290	247.08(11)	26(2)	23984	27(3)	0	<0.30	
2172.43(15)	1290	882.80(11)	100	219859	29(2)	0	<0.20	15.6(7) [g]
2233.26(16)	1537	696.54(13)	100	53798	−70(6)	14(5)	0.55(3)	0.53(9)
2705.92(18)	2172	533.49(11)	100	12892	18(4)	11(4)	<0.30	3.2(1.0) [g]
2826.60(19)	1537	1289.88(N) [h]	≤7	<1500	···	···	···	0.10(6)
	2233	593.33(10)	≥93	19508	53(5)	0	0.92(2)	
3084.25(18)	2172	911.81(11)	99.3(3)	140057	29(3)	−3(3)	<0.20	>1.8
	2706	377.97(26)	0.7(3)	996	53(10)	0	···	
3243.68(18)	2172	1071.24(11)	100	21500	−47(3)	0	0.76(3)	0.25(6)
3592.34(50)	2827	765.73(41)	100	22575	−51(3)	0	0.98(3)	<0.10
4349.69(50)	3592	757.35(16)	100	13852	−35(6)	8(7)	1.03(3)	<0.10
4697.06(30)	3084	1612.78(12)	100	68908	35(2)	−11(3)	0.70(4)	0.32(8)
5001.52(60)	3084	1917.23(53)	100	18584	4(3)	0	1.08(10)	<0.10

[a] Deduced from the γ-ray energies of column 3, including corrections for nuclear recoil. Throughout this table, the figures in parentheses are the uncertainties in the least significant figure. Only levels formed directly in the present studies are included.

[b] Not corrected for nuclear recoil.

[c] Results of fitting the ^{9}Be + ^{48}Ca angular distributions at $E(^{9}\text{Be}) = 27$ MeV with the Legendre polynomial $W(\theta) = I_\gamma[1 + A_2P_2(\cos\theta) + A_4P_4(\cos\theta)]$. An entry of 0 for A_4 means the fit was to $I_\gamma[1 + A_2P_2(\cos)]$. The γ-ray intensity I_γ has been corrected for the variation in the detector efficiency.

[d] The DSAM attenuation coefficient defined in Ref. 1.

[e] Level mean life deduced from $F(\tau)$ as discussed in Ref. 1.

[f] From Ref. 6.

[g] Reference 6 (Radford and Poletti).

[h] Not observed. The nominal energy is calculated from the energy level separation.

II. DECAY SCHEMES

A. ^{53}Cr

^{53}Cr, formed via the ^{48}Ca(^{9}Be, $4n$)^{53}Cr reaction, and ^{54}Cr were the most intensely produced nuclei in ^{9}Be + ^{48}Ca at 20–45 MeV. The results obtained for ^{54}Cr have already been reported.[3] The γ rays listed in Table I were identified with ^{53}Cr and sorted into the decay scheme of Fig. 1 using the γ-γ–coincidence data in conjuction with the relative intensity, angular distribution, and DSAM lifetime information, i.e., $F(\tau)$ values, listed in Table I. The 90° spectrum from the ^{9}Be + ^{48}Ca angular distribution measurements is shown in Fig. 2. Recoil distance method (RDM) lifetime measurements were not made for ^{9}Be + ^{48}Ca.

The levels shown in Fig. 1 and listed in Table I were all observed previously via the ^{51}V(^{7}Li, αn)^{53}Cr reaction[4] except for the 4350- and 5002-keV levels which have not been previously reported. The 1613- and 1917-keV deexcitation γ rays from these levels (see Fig. 1) are clearly evident in the data of Fig. 2. The present results are in good agreement with the previous ^{51}V + ^{7}Li results except for the interpretation of the 1613-keV 4697 → 3084 transition as discussed below.

Only the ^{53}Cr levels observed in ^{48}Ca + ^{9}Be are shown in Fig. 1 and Table I. Of these, the first four[6] excited states have well-established spin-parities and γ-ray branching ratios and, although the mean-life information for these levels is sparse and/or contradictory,[6] we have nothing worthwhile to add. (A recent study[6] has, however, put three of the four lifetimes on a firmer footing.) The DSAM lifetime of 0.53 ± 0.09 ps obtained in the present study for the 2233-keV level is in good agreement with the previous value[4] of $0.4^{+0.4}_{-0.15}$ ps. Except for the 3084-keV level,[4] there was no previous lifetime information for any of the levels of Table I above 2500-keV excitation.[6]

The 2706- and 3244-keV levels observed by Poletti *et al.*,[4] but listed as questionable in the latest compilation,[6] are definitely corroborated by the present studies and the studies of Radford and Poletti.[6] The nonobservation of the 2706-keV level in pre-

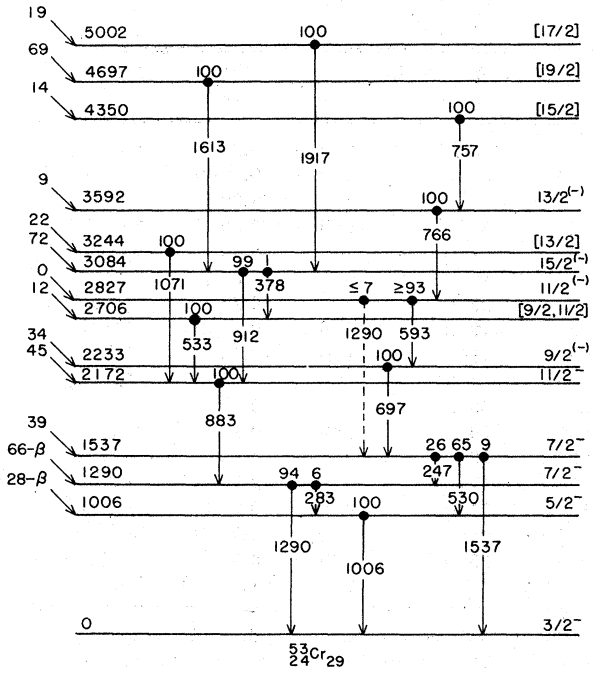

FIG. 1. Level scheme for ^{53}Cr deduced from present studies of the ^{48}Ca(^{9}Be, $4n$)^{53}Cr reaction. The only energy levels shown are those derived from the γ-ray transitions observed in ^{9}Be+ ^{48}Ca and indicated in the figure. Excitation and transition energies are in keV and branching ratios are in percent. The spin-parity assignments in square brackets are from the present work and are speculative, the remainder are from the compilation of Ref. 6. The observed level side feeding in ^{9}Be+ ^{48}Ca at $E(^{9}\text{Be}) = 27$ MeV is shown at the left.

vious ^{50}Ti(α, n)^{53}Cr studies[6] is probably due to the masking of its 533-keV decay γ ray by the much more intense 530-keV γ ray deexciting the 1537-keV level. The lifetime observed for the 3244-keV level is too short for anything but decay via dipole radiation. Hence the spin of this level is restricted to $\frac{9}{2}$-$\frac{13}{2}$; both the angular distribution and the reaction mechanism, which preferentially populate yrast levels,[1-3] favor $J = \frac{13}{2}$. Similarly, the 4350-keV level appears to decay by a fast $J+1 \rightarrow J$ dipole transition to the $J = \frac{13}{2}$ 3592-keV level. Hence we have a definite restriction $J = \frac{11}{2}$-$\frac{15}{2}$ and a probable $J = \frac{15}{2}$ assignment for the 4350-keV level. Likewise, the 5002 → 3084 transition is fast enough to be almost certainly dipole, hence $J = \frac{13}{2}$-$\frac{17}{2}$ and most probably $\frac{17}{2}$. However, the angular distribution is not consistent with a $J+1 \rightarrow J$ dipole transition and would appear to be mixed $E2/M1$ if $J = \frac{17}{2}$.

For the 1613-keV 4697 → 3084 transition, the ^{48}Ca + ^{9}Be results give a firm preference for a quadrupole $J+2 \rightarrow J$ transition, which we assume. However, we note the previous ^{51}V + ^{7}Li results[4] are in disagreement with this assignment. Likewise, the present DSAM results are in disagreement with the previous ^{51}V + ^{7}Li study which gave $F(\tau) < 0.10$, hence $\tau > 0.8$ ps. There is no doubt of the present result of $F(\tau) = 0.70 \pm 0.04$ since the result—originally obtained in the angular distribution studies—was confirmed by the γ-γ-coincidence data. We note that the 1613-keV γ ray was relatively considerably weaker in the ^{51}V(^{7}Li, αn)^{53}Cr reaction.

B. ^{54}V

The nucleus ^{54}V was formed, albeit weakly, in the ^{48}Ca(^{9}Be, $2np$)^{54}V reaction. The more prominent γ rays from ^{54}V are identified in Fig. 2, and the results are summarized in Fig. 3 and Table II. ^{54}V is quite difficult to reach and the only information on its level scheme reported in the compilations[7] is a very recent ^{54}Cr(t, ^{3}He)^{54}V study.[8] The level scheme obtained in this study is also shown in Fig. 3, although no information on spins or parities was reported.

The decay scheme shown on the right in Fig. 3 was deduced as the most probable one from the γ-γ-coincidence data, taken at $E(^{9}\text{Be}) = 35$ MeV, and the angular distribution data summarized in Table II. After comparison with the (t, ^{3}He) results, the bottom level in this scheme was identified with the ^{54}V ground state rather than the level at 111 ± 8 keV for four reasons: (1) No γ ray of energy 111 ± 8 keV was observed in the present work and only one half-life component has been observed[7,9] in ^{54}V(β^-)^{54}Cr. (2) From its intensity the 245-keV γ ray can be placed at the bottom of the decay scheme, and no level of $111 + 245 = 356$ keV was observed in the (t, ^{3}He) study. (3) A level of 238 ± 8 keV observed in (t, ^{3}He) can be identified with a 245-keV level deduced from the present results. (4) As previously discussed,[9] there is good balance in intensity between the 245-keV γ ray and the ^{54}V(β^-)^{54}Cr transitions observed simultaneously.

Although it is clear from γ-γ-coincidence data that the γ rays of 245, 970, 615, and 469 keV form a cascade chain, the order of the latter three is uncertain. Thus, as shown in Fig. 3 and Table II, the 245- and 2298-keV levels of ^{54}V are the only two which we consider as definite and the high-spin ^{54}V level scheme we present here is only the most probable. Because of the presence of the crossover transitions $1585 = 615 + 970$ and $1084 = 615 + 469$, the 615-keV transition is definitely placed between the 469- and 970-keV transitions. The relative intensities observed in the singles measurements then suggest the order given in Fig. 3, although the results are somewhat less

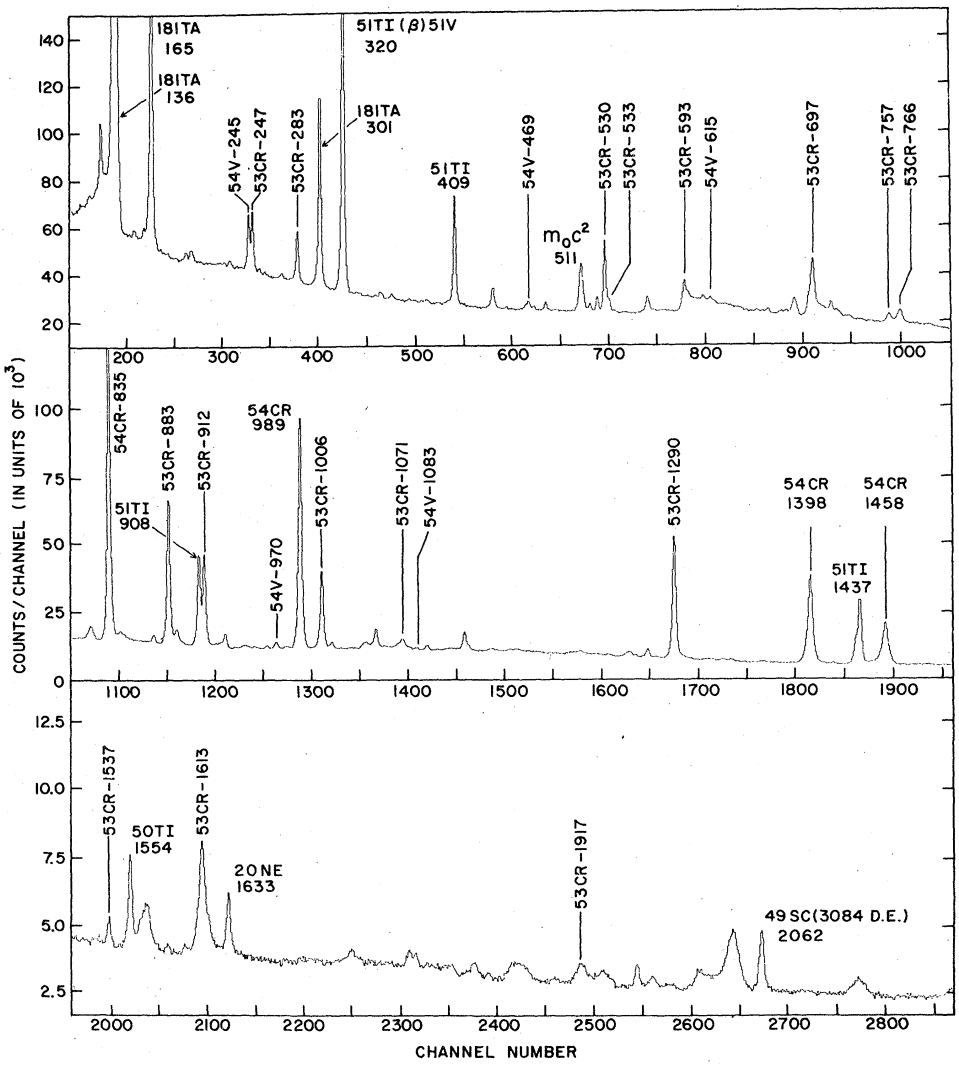

FIG. 2. Segment of a 4096-channel Ge(Li) spectrum measured at $\theta_\gamma = 90°$ in the ^{9}Be+ ^{48}Ca angular distribution measurements. These data were recorded for $E(^9\text{Be}) = 27$ MeV at a dispersion of 0.774 keV/channel. The ^{53}Cr and ^{54}V lines are labeled by the nucleus and the transition energy (given in keV). The assignments of these lines to specific transitions in ^{53}Cr and ^{54}V are given in the text and subsequent figures. The stronger lines from ^{49}Sc, ^{50,51}Ti, and ^{54}Cr are also labeled; the ^{181}Ta lines result from Coulomb excitation of the tantalum backing.

than conclusive. It is thus quite possible that the 469- and 970-keV transitions should be interchanged, although this implies a rather unusual set of side feedings for the higher-lying levels. Supporting evidence for the scheme illustrated was also obtained from the γ-γ-coincidence data. In particular, the relative intensities of the various γ rays observed in coincidence with the 245 $\rightarrow$ 0 transition are in quite reasonable agreement with the level ordering given in Fig. 3, whereas for the alternative case marked disagreements (factors 2–4) were noted.

Regardless of the ordering of the four cascade γ rays of 245, 970, 615, and 469 keV, all have angular distributions consistent with $J+1 \rightarrow J$ dipole transitions and so the yrast scheme is most probably J, $J+1$, $J+2$, $J+3$, and $J+4$. A model-dependent argument that the ^{54}V ground state has $J^\pi = 3^+$ has previously been given,[9] based on shell-model calculations and ^{54}V(β)^{54}Cr results. The predicted ^{54}V yrast scheme shown in Fig. 3 will be discussed in Sec. III.

C. ^{62}Co

Results for ^{62}Co obtained in the ^{48}Ca(^{18}O, $3np$)^{62}Co reaction are collected in Fig. 4 and Table III. Also shown in Fig. 4 is the level scheme deduced

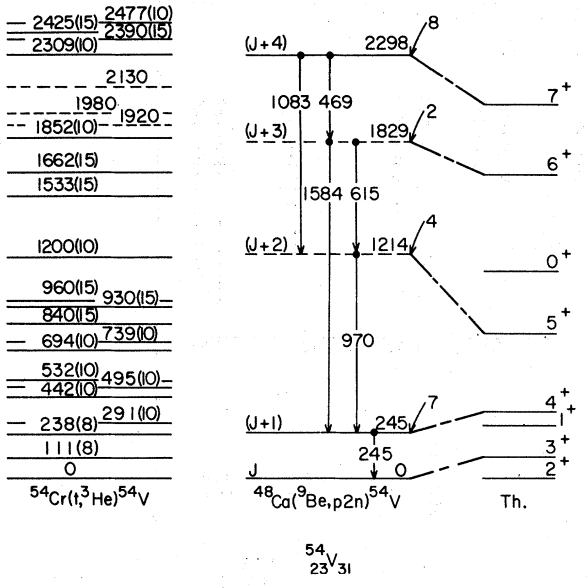

FIG. 3. Level scheme for ^{54}V deduced from present studies of the ^{48}Ca(^{9}Be, $2np$) ^{54}V reaction (middle) and previous studies of the ^{54}Cr(t,^{3}He) ^{54}V reaction (left). Excitation and transition energies are in keV and for the (t,^{3}He) results the uncertainty is given in parentheses. Dashed levels indicate most probable assignments (see text). The relative side-feeding intensity in ^{9}Be+ ^{48}Ca is indicated on the right of the γ-decay scheme. In the present work the spins of the higher-lying levels are obtained relative to that of the ground state. From model-dependent arguments (see Ref. 9) the most likely value for this spin is $J=3$. The theoretical yrast spectrum on the far right is a shell-model prediction discussed in Sec. III.

from the ^{62}Ni(t, ^{3}He)^{62}Co reaction.[11] From these (t, ^{3}He) results, ^{64}Ni(d,α)^{62}Co angular distributions,[12] and studies[10] of ^{62}Co(β^-)^{62}Ni it is concluded that the ^{62}Co ground state has $J^\pi=1^+$ or 2^+ and β decays with a 1.5-min half-life, while one member of a possible doublet at 22 ± 5 keV excitation has $J^\pi=4^+$ or 5^+ and β decays with a 13.9-min half-life.[10] We would expect the high-spin isomer at 22 ± 5 keV to be fed strongly in ^{18}O + ^{48}Ca and, as can be seen in Fig. 4, there is a good match in excitation energies of our scheme to the (t, ^{3}He) scheme if we assume the bottom level in our scheme is in fact at 22 keV. Moreover, in this adopted match of the two schemes all the suspected[11] high-spin ($J\gtrsim5$) levels from the (t, ^{3}He) results are involved.

The (t, ^{3}He) angular distribution results are stated[11] to favor $J^\pi=5^+$ for one member of the 22-keV doublet, while the (d,α) results are stated[12] to favor $J^\pi=5^+$ for the 613-keV level. In this case we postulate that the value of J which appears in Fig. 4 is $J=5$: the high-spin level scheme therefore has spins, in order of increasing excitation, of 5-5-6-7-8. We note that the mean lives obtained (Table III) for the upper two transitions are too fast to be anything but dipole,[13] and although the angular distributions permit both $J-1\rightarrow J$ and $J+1\rightarrow J$ for the 767-, 327- and 1194-keV transitions, the side-feeding intensities favor the latter. Note that the $J=7$ assignment suggested for the 1546-keV level is not in agreement with the (t, ^{3}He) results for a reported 1542-keV level (which we believe is the same state), for which the conclusion was $J^\pi=(5^+,6^+)$.

TABLE II. The most-probable γ-decay scheme of ^{54}V from ^{48}Ca(^{9}Be, $p2n$)^{54}V.

E_i [a] (keV)	E_f (keV)	E_γ [b] (keV)	Angular distribution [c] I_γ	A_2 (%)	Branching ratio (%)	$F(\tau)$ [d]	τ [e] (ps)
244.65(11)	0	244.65(11)	17432	−18(11)	100	<0.5	···
1214.58(19)	245	969.92(15)	6729	−45(4)	100	<0.3	···
1829.23(36)	1215	614.89(60)	3200	−29(12)	48(15)	<0.4	···
	245	1584.46(40)	3500	···	52(15)	···	
2298.00(26)	1829	469.11(20)	4548	−36(4)	58(10)	<0.5	>0.5
	1215	1083.04(30)	3257	+81(20)	42(10)	···	

[a] Deduced from the γ-ray energies of column 3, including corrections for nuclear recoil. Throughout this table, the figures in parentheses are the uncertainties in the least significant figure. Only levels formed directly in the present studies are included.

[b] Not corrected for nuclear recoil.

[c] Results of fitting the ^{9}Be+ ^{48}Ca angular distributions at $E(^{9}\text{Be})=27$ MeV with the Legendre polynomial $W(\theta)=I_\gamma[1+A_2P_2(\cos\theta)+A_4P_4(\cos\theta)]$. The A_4 coefficients were not determined with significant accuracy to distinguish them from zero.

[d] The DSAM attenuation coefficient defined in Ref. 1.

[e] Level mean life deduced from $F(\tau)$ as discussed in Ref. 1.

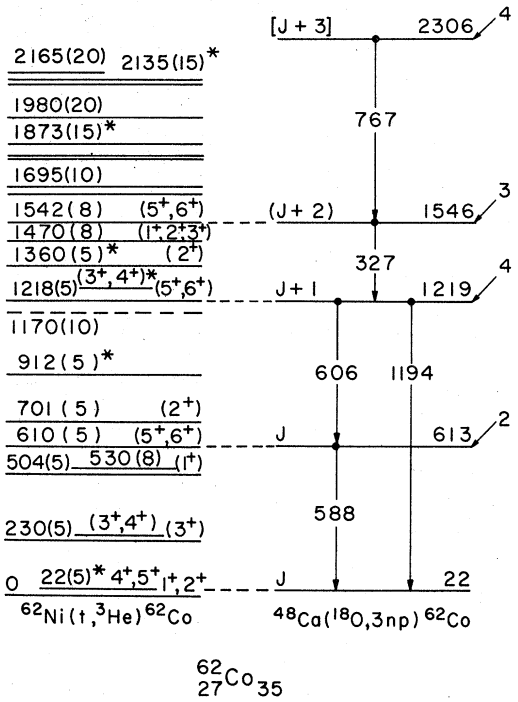

$^{62}_{27}Co_{35}$

FIG. 4. Level scheme for ^{62}Co deduced from present studies of the ^{48}Ca(^{18}O, $3np$) ^{62}Co reaction (right) and previous studies of the ^{62}Ni(t, ^{3}He) ^{62}Co reaction (left). Excitation and transition energies are in keV and for the (t, ^{3}He) results the uncertainty is given in parentheses. Those levels which are suspected doublets are indicated by an asterisk. On the left, the spin-parities for the 0- and 22-keV levels are from β-decay results (see Ref. 10), and the remaining (uncertain) assignments are from the (t, ^{3}He) study of Ref. 11. The relative side-feeding intensity in ^{18}O+ ^{48}Ca is indicated on the far right. The best overlap of the present results with the (t, ^{3}He) work is obtained if the lowest-lying level in the observed γ-ray cascade is matched with the 22-keV level. In the present work the spins of the higher-lying-levels are obtained relative to that of the 22-keV level. From a comparison of the present and previous results the most probable value for J, the spin of the 22-keV level, is 5.

D. ^{61}Ni

High-spin states of ^{61}Ni have been studied extensively in recent investigations of the ^{58}Fe($\alpha, n\gamma$)^{61}Ni and ^{53}Cr(^{11}B, $2np\gamma$)^{61}Ni reactions. Our results add very little which is new but are given here briefly because they illustrate once again the high selectivity of the HI fusion-evaporation reaction for high-spin states. The results are collected in Table IV which lists the states which were populated directly in the present studies. As can be seen from the previous spin-parity assignments (column 2 of Table IV), the observed levels have spins increasing with excitation energy and are, according to the conclusions of Wadsworth *et al.*,[14] the yrast levels of ^{61}Ni. Our results are in all respects consistent with the much more detailed data of Wadsworth *et al.*, who observed 18 levels below an excitation energy of 2150 keV in ^{61}Ni as opposed to the 4 included in Table IV. (However, some very weak transitions from non-yrast levels observed in the present study are not included in Table IV.) The only new information of interest is the mean-life limit, $\tau < 1.5$ ps, for the 4810 → 4020 transition. This is fast enough to ensure a predominantly dipole transition and so supports the conjectured $J = \frac{17}{2}$ assignment for the 4818-keV level.

E. ^{62}Ni

^{62}Ni was formed strongly in the ^{48}Ca(^{18}O, $4n$)^{62}Ni reaction at 40–55-MeV bombarding energy. The data on γ-ray energies, angular distributions, and Doppler-shift-attenuation factors for transitions associated with ^{62}Ni are given in Table V. The resulting decay scheme deduced from these data is shown in Fig. 5, and a summary of level properties for states observed in the present work, including excitation energies, J^π values, γ-ray branching ratios, lifetimes, mixing ratios, and reduced transition strengths, is presented in Table VI.

The four levels below 4-MeV excitation energy can all be associated with previously reported levels.[10,16] The $J^\pi = 2^+$ and 4^+ assignments to the 1173- and 2336-keV levels are from Coulomb excitation and ^{60}Ni(t, p)^{62}Ni studies, respectively,[10] while the assignments for the 3176- and 3277-keV levels are based on the ^{64}Ni(p, t)^{62}Ni reaction alone.[16] These previous assignments are consistent with and supported by the present angular distribution measurements on the decay γ rays.

The 4018-keV level is probably identical to a level reported at 4011 ± 5 keV, which was weakly populated in the ^{64}Ni(p, t)^{62}Ni and ^{61}Ni(d,p)^{62}Ni reactions.[16,10] The level was tentatively assigned $l = (3)$ in unpublished ^{61}Ni(d,p)^{62}Ni results,[17] and hence $J^\pi = (1^+ - 5^+)$. However, the usual arguments[1-3] concerning the reaction mechanism, lifetimes, and angular distributions strongly suggest a 6^+ assignment for the 4018-keV level. For example, the angular distribution of the 4018 → 2336 transition is in agreement with that expected for $\Delta J = 2$; if $J = 6$, the 4018-keV level lifetime demands $E2$ for this transition and hence $J^\pi = 6^+$. Finally, the intense feeding of this level strongly suggests it is an yrast level, i.e., $J \geq 5$. In view of the tentative nature of the (d,p) work, we adopt (6^+) as the J^π of this level.

The level at 4160 keV may correspond to one

TABLE III. γ decay of ^{62}Co from ^{48}Ca(^{18}O, $3np$)^{62}Co.

E_i[a] (keV)	E_f (keV)	E_γ[b] (keV)	Angular distribution[c] I_γ	A_2 (%)	Branching ratio (%)	$F(\tau)$[d]	τ[e] (ps)
22.0(5.0)[f]	0	...	...	...	...	...	
609.71(14)	22[g]	587.71(14)	4625	−63(7)	100	...	
1216.30(15)	610	606.44(15)	2782	−91(40)	25(4)	...	
		1194.45(18)	8279	−34(6)	75(4)		
1543.22(19)	1216	326.92(12)	6887	−59(4)	100	0.21(2)	1.9(4)
2309.72(90)	1543	766.50(90)	~4000	...	100	>0.60	<0.40

[a] Deduced from the γ-ray energies of column 3, including corrections for nuclear recoil. Throughout this table, the figures in parentheses are the uncertainties in the least significant figure. Only levels formed directly in the present studies are included.

[b] Not corrected for nuclear recoil.

[c] Results of fitting the ^{18}O+^{48}Ca angular distributions with the Legendre polynomial $W(\theta)=I_\gamma[1+A_2P_2(\cos\theta)+A_4P_4(\cos\theta)]$. The A_4 coefficients were not determined with significant accuracy to distinguish them from zero.

[d] The DSAM attenuation coefficient defined in Ref. 1.

[e] Level mean life deduced from $F(\tau)$ as discussed in Ref. 1.

[f] From Ref. 10.

[g] Assumed value.

TABLE IV. γ decay of ^{61}Ni from ^{48}Ca(^{18}O, $5n$)^{61}Ni.

E_i[a] (keV)	J_i^π[b]	E_f (keV)	E_γ[c] (keV)	Angular distribution[d] I_γ	A_2 (%)	Branching ratio (%) Previous[b]	Present	τ (ps) Previous[b]	Present
67.415(10)[e]	$\frac{5}{2}^-$	0		...	...	...	100	...	
1015.20(15)	$\frac{7}{2}^-$	67	947.86(16)	15709	42(3)	75(1)	≥59	9(2)	6.4(8)[f]
		0	1015.11(17)	≤11000[g]	21(3)	25(1)	≤41		
2121.76(23)	$\frac{9}{2}^+$	1015	1106.55(18)	13475	−21(3)	100	100	>0.5	
2129.28(23)	$\frac{11}{2}^-$	1015	1114.08(18)	6133	47(9)	100	100	>3.0	
3426.88(37)	$\frac{13}{2}^-$	1807	1618.9(5)[b,h]	...	...	21(2)	...	>1.0	
		1987	1438.41(15)	6955	...	69(3)	...		
		2129	1297.5(5)[b,h]	...	...	10(1)	...		
3435.81(30)	$\frac{13}{2}^+$	2122	1314.04(20)	5194	1(10)	100	100	1.4(5)	<2.0[f]
4019.84(34)	$\frac{15}{2}^+$	3436	584.03(15)	2082	29(13)	28(3)	34(5)	>2.0	
		3426	592.96(14)	3922	−63(7)	72(3)	66(5)		
4819.24(60)	$(\frac{17}{2}^+)$	4020	799.4(5)[b]	~3000	...	100	100	...	<1.5[i]

[a] Deduced from the γ-ray energies of column 4, including corrections for nuclear recoil. Throughout this table, the figures in parentheses are the uncertainties in the least significant figure. Only levels formed directly in the present studies are included. Weakly formed levels with excitation energies between 900 and 2100 keV have been omitted.

[b] Reference 14.

[c] Not corrected for nuclear recoil.

[d] Results of fitting the ^{18}O+^{48}Ca angular distribution with the Legendre polynomial $W(\theta)=I_\gamma[1+A_2P_2(\cos\theta)+A_4P_4(\cos\theta)]$. The A_4 coefficients were not determined with significant accuracy to distinguish them from zero.

[e] Reference 15.

[f] From a RDM result (see Ref. 1).

[g] Unresolved from a contaminant γ ray.

[h] Observed in coincidence only.

[i] Based on the DSAM result, $F(\tau)>0.3$ (see Ref. 1).

member of a possible doublet observed at 4154 ± 6 keV in the ^{64}Ni$(p,t)^{62}$Ni reaction and assigned $L=(4)$, hence $J^\pi=(4^+)$.[16] However, the angular distributions of the γ-ray decays to the 4_1^+ and 4_3^+ levels (1825- and 884-keV transitions, respectively) rule against a $J\to J$ transition and instead favor $\Delta J=\pm 1$. The reaction mechanism, of course, favors $J+1\to J$ and therefore we conclude $J^\pi=(5)^{\pi_0}$, where the parity π_0 cannot be determined from the present data.

The remaining levels in Table VI have not been previously reported. It was not possible to determine the parity of these levels although it was sometimes possible to determine the parity *relative* to π_0 (parity of the 4160-keV level). The $J^\pi=(7^{\pi_0})$ assignment to the 4648-keV level follows from the $\Delta J=1$ and $\Delta J=2$ angular distribution patterns for the decay to the (6^+) and (5^{π_0}) levels, respectively, as well as the transition strength to the (5^{π_0}) level, which rules out $M2$ radiation.[13] Similarly we assign $J^\pi=(9^{\pi_0})$ to the 5751-keV level based on the $\Delta J=2$ pattern and the transition strength for the decay to the (7^{π_0}) level. The $J^\pi=(11^{\pi_0})$ and (9^{π_0}) assignments to the 7559- and 6647-keV levels follow from the $\Delta J=2$ nature of the 7559 → 5751 and 7559 → 6647 transitions, respectively, and as before the lifetimes rule out $M2$ transitions so that $\pi=\pi_0$. Unfortunately, the angular distributions of the γ rays depopulating the 6647-keV level were not sufficiently definitive

TABLE V. γ rays from ^{62}Ni observed in ^{48}Ca(^{18}O, $4n$) ^{62}Ni at 50 MeV.

E_γ[a] (keV)	Angular distribution[b] I_γ	A_2 (%)	A_4 (%)	$F(\tau)$[c]
487.59(13)	46187	19(2)	−13(2)	
630.00(14)	89000[d]	−33(2)	0	
702.02(14)	19031	···	···	
883.54(16)	17005	−33(2)	0	
895.75(16)	9614	···	···	
912.33(16)	5622	28(7)	0	
1102.41(17)	43726	30(5)	0	0.53(10)
1157.24(22)	9962	···	···	
1163.30(18)	211570	16(2)	−9(3)	
1172.72(18)	258374	19(2)	−9(2)	
1402.05(21)	5661	···	···	>0.8
1530.43(21)	6932	···	···	
1682.34(21)	108938	21(2)	−8(2)	0.22(15)
1808.43(22)	12257	10(3)	0	0.25(8)
1824.66(22)	59544	−30(2)	0	
1997.94(24)	8491	···	···	
2003.25(25)	10270	10(5)	0	
2103.78(25)	19489	17(4)	0	
2490.92(34)	4207	···	···	
2571.30(30)	3477	···	···	

[a] Uncorrected for nuclear recoil. Throughout this table, numbers in parentheses are errors in the least significant figure.

[b] Results of fitting ^{18}O+^{48}Ca angular distributions with the Legendre polynomial function $W(\theta)=I_\gamma[1+A_2P_2(\cos\theta)+A_4P_4(\cos\theta)]$. An entry of 0 for A_4 means the fit was to $I_\gamma[1+A_2P_2(\cos\theta)]$.

[c] The DSAM attenuation factor defined in Ref. 1.

[d] A 10% contribution from a contaminant γ ray in ^{63}Ni has been subtracted, as discussed in the text.

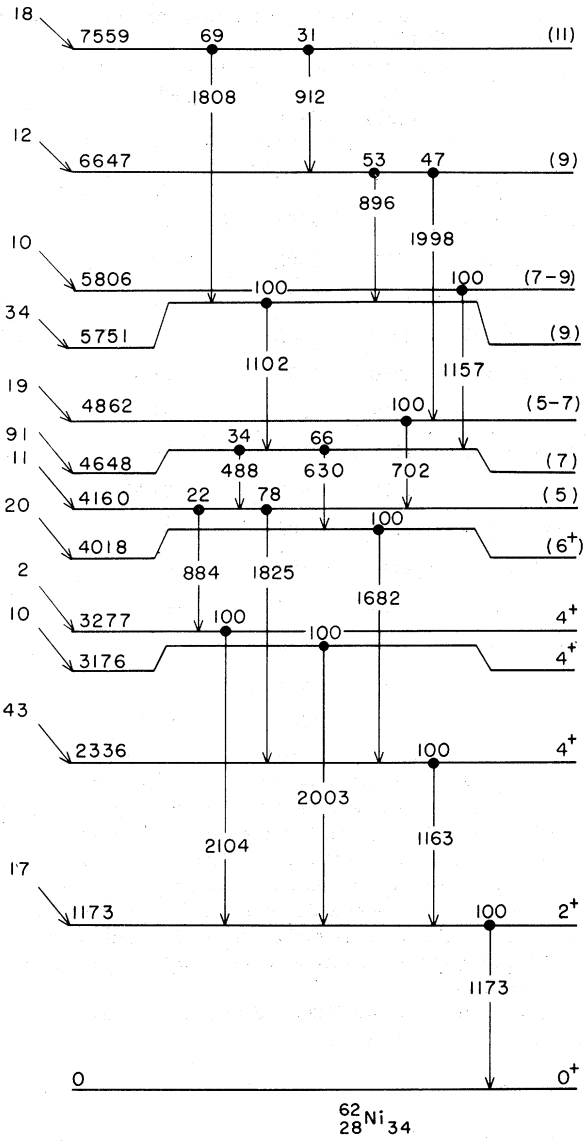

FIG. 5. Level scheme for ^{62}Ni deduced from present studies of the ^{48}Ca(^{18}O, $4n$) ^{62}Ni reaction. Excitation energies and transition energies are in keV and branching ratios are in percent. Relative side-feeding intensities are indicated on the left. Spin-parity assignments enclosed in parentheses indicate probable but uncertain conclusions, as discussed in the text.

TABLE VI. Energy levels, lifetimes, and γ-ray branching ratios and transition strengths for ^{62}Ni deduced from the ^{48}Ca(^{18}O, $4n$) ^{62}Ni studies.

E_i [a] (keV)	E_f (keV)	E_γ (keV)	Branching ratio (%)	J_i^π	J_f^π	Mixing ratio x [b] (× 100)	Mean life (ps)	$B(E2)$ [c] (W.u.)
1173.00(7)	0	1173	100	2^+	0^+	$E2$	2.09(3) [d] 1.6(5) [e]	11.8(2) 15^{+3}_{-3}
2336.22(19)	1173	1163	100	4^+	2^+	$E2$	<3 $1.5^{+1.0}_{-0.5}$ [e]	>8.5 17(8)
3176.42(22)	1173	2003	100	4^+	2^+	$E2$		
3277.09(22)	1173	2104	100	4^+	2^+			
4018.38(33)	2336	1682	100	(6^+)	4^+	$E2$	0.9(4)	4.5(2.0)
4160.41(45)	2336	1825	78(4)	(5^{π_0}) [e]	4^+	−0.16(6) −3.1(4)	<2	>0.03 >0.95
	3277	884	22(1)		4^+	−0.24(6) −2.4(4)		>0.61 >9.5
4648.38(36)	4018	630	66(7)	(7^{π_0})	(6^+)	−0.19(4) −2.3(5)	734(34)	0.026(1) 0.63(3)
	4160	488	34(3)		(5^{π_0})	$E2$		0.9(1)
4862.43(47)	4160	702	100	$(5,6,7^{\pi_0})$	(5^{π_0})		12.1(2)	26.5(4)
5750.80(40)	4648	1102	100	(9^{π_0})	(7^{π_0})		0.8(3)	42(16)
5805.63(42)	4648	1157	100	$(7,8,9^{\pi_0})$	(7^{π_0})		<2	>13
6646.61(50)	5751	896	53(5)	(9^{π_0})	(9^{π_0})			
	4648	1998	47(4)		(7^{π_0})			
7559.26(46)	5751	1808	69(6)	(11^{π_0})	(9^{π_0})		1.2(6)	1.6(8)
	6647	912	31(3)		(9^{π_0})			22(11)

[a] Corrected for nuclear recoil. The first four levels are weighted means of energies from the present and previous studies (Refs. 10,16), while the remaining are from the present work only.

[b] The $E2/M1$ mixing ratio x was determined from the γ-ray angular distributions, using the 1173- and 1163-keV transitions to fix the A_2 attenuation factor, α_2, at 0.28.

[c] The reduced $E2$ strength determined from the mean life, branching ratio, and multipole mixing ratio. In cases where no mixing ratio is given, pure $E2$ radiation is assumed.

[d] From Coulomb excitation studies summarized in Ref. 10.

[e] Reference 18.

[f] The parity π_0 of the 4160-keV level and all higher levels are not determined, but for some higher levels the parity is determined *relative* to π_0.

to provide confirming information. Finally, a combination of lifetime information and the usual yrast arguments were used to limit the spins of the 4862- and 5806-keV levels to (5–7) and (7–9), respectively.

The mean life of the 1173-keV 2^+ level has been determined from Coulomb excitation studies,[10] and we provide no new information. Other lifetimes in Table VI come mainly from the RDM experiment although some limited DSAM information was available. The decays of levels fed by the $J=(7)$ 4648-keV state are dominated by the rather slow (734 ps) mean life of that level. However, in several cases there was sufficient direct feeding to extract a lifetime. For the 4018-keV (6^+) level, the observation of a Doppler-shifted component at the smallest distance (10 μm) allows an upper limit of 1.3 ps (see Fig. 6), whereas the DSAM data from the γ-γ experiment allows the lower limit of 0.5 ps. These limits are combined to give $\tau = 0.9 \pm 0.4$ ps. Similarly, the RDM and DSAM combined to give results of 0.8 ± 0.3 and 1.2 ± 0.6 ps for the mean lifes of the 5781- and 7559-keV levels, respectively. For the 4160- and 2336-keV levels, there was an additional 12.1 ± 0.2-ps component from the decay of the 4862-keV level (see Fig. 6), and after correcting for this feeding, we find $\tau < 2$ ps and $\tau < 3$ ps, respectively. This result for the 2336-keV level is in agreement with a recent DSAM measurement[18] of $1.5^{+1.0}_{-0.5}$ ps. Similarly, the RDM measurement on the 1157-keV γ ray allows the limit $\tau < 2$ ps for the 5806-keV level. Finally, we note that it was possible to separate out a short-lived ($\tau < 1$ ps) 630-keV transition due to ^{63}Ni from the longer-lived ($\tau = 734$ ps) 630-keV transition of

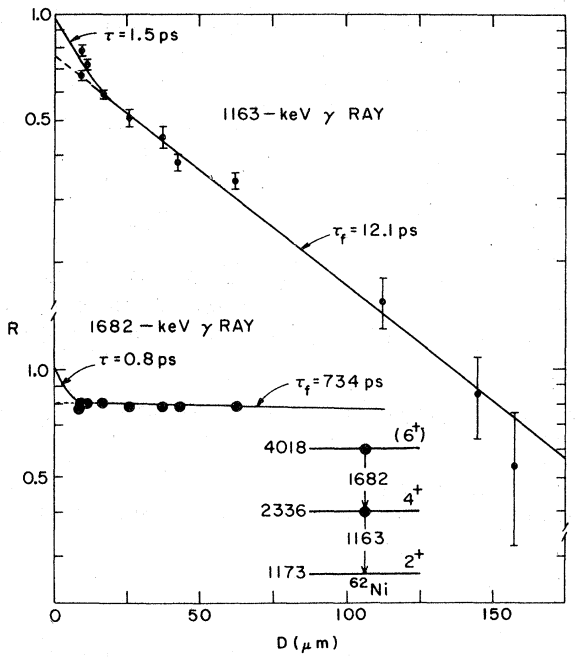

FIG. 6. RDM lifetime results for the ^{62}Ni 1163-keV 2336→1173 transition and 1682-keV 4018→2336 transition. R is the fraction of the total γ-ray intensity contained in the unshifted component and is plotted as a function of plunger distance $D=vt$, where v is the recoil ion velocity. Thus R should decay as $e^{-D/v\tau}$, where τ is the mean life associated with the decay. For the 1682-keV transition, the observed decay follows that of a long-lived ($\tau_f=734$ ps) feeding level (see Table VI and the dashed curve indicates the extrapolation of that decay to zero flight time. The nonunity intercept implies an additional short-lived component and allows the limit $\tau<1.3$ ps. The solid curve is that expected for $\tau=0.8$ ps. For the 1163-keV transition, the 734-ps component has already been subtracted. The remainder follows the decay of a 12.1-ps feeding level (see Table VI), which is extrapolated to zero flight time by the dashed line. The nonunity intercept again indicated an additional short-lived component and allows the limit $\tau<3$ ps. The solid curve is that expected for $\tau=1.5$ ps.

^{62}Ni using the RDM data at the closest distance, where the Doppler-shifted component is due entirely to ^{63}Ni (see Tables V and VII).

F. ^{63}Ni

^{63}Ni was formed by the ^{48}Ca(^{18}O, $3n$)^{63}Ni reaction. Since the low-lying level scheme is well known[19] it was relatively easy to fit the observed γ-γ-coincidence data into a level scheme. The γ-decay results are collected in Table VII and the decay scheme is shown in Fig. 7. The first two excited states of Fig. 7 were observed previously[19] and given the spin-parity assignments shown. Our results support the most-probable assignment $\frac{9}{2}^+$ to the 1292-keV level since the 1292→87 transition has a characteristic $J+2\rightarrow J$ angular distribution and the very long lifetime favors $M2$ radiation (0.23 W.u.) over $E2$ radiation (4.4×10^{-3} W.u.). The most-probable spin-parity of $\frac{11}{2}^+$ or $\frac{13}{2}^+$ for the 2184-keV level follows from the strong feeding of this level and the 2184→1292 angular distribution results, which together suggest the transition is either $E2/M1$-mixed $J+1\rightarrow J$ or a pure $E2$ $J+2\rightarrow J$ transition: the mean life of 5.2 ps rules out a significant $M2$ contribution since it would correspond to 1.1×10^3 W.u. The spin-parity of $\frac{13}{2}^+$ conjectured for the 2814-keV level is based solely on the angular distribution of the 2814→1292 transition. Unfortunately, the 631-keV 2814→2184 transition was obscured by the much more intense ^{62}Ni 630-keV transition so that its angular distribution could not be obtained. However, in the RDM measurement a fraction of the 630-keV γ-ray intensity—ascribable to the ^{63}Ni 2814→2184 transition—was observed to have a much shorter lifetime ($\tau<1$ ps) than the main ^{62}Ni component. The RDM and DSAM limits for the 2814-keV level (Table VII) result in a lifetime of 0.7 ± 0.3 ps consistent with decay modes of $M1$ and $E2$ to the 2814→2184 and 2814→1292 transitions, respectively. The latter transition is too fast to be $M2$; hence the postulated $\frac{13}{2}^+$ assignment to the 2814-keV level.

III. DISCUSSION

A. ^{53}Cr

The previous ^{53}Cr results[4] from the ^{51}V(^{7}Li, αn)^{53}Cr reaction were compared in detail to predictions of Horie and Ogawa[20] for the configurational space

$$[(\pi 1f_{7/2})^n \otimes (\nu 2p_{3/2}, 1f_{5/2}, 2p_{1/2})^m], \qquad (1)$$

with $n=4$, $m=1$. The predicted yrast $\frac{13}{2}^-$, $\frac{17}{2}^-$, and $\frac{19}{2}^-$ states were not identified in the previous work. With our more accurate angular distribution data, likely candidates for these yrast states have been located at 3244, 5002, and 4697 keV. Likewise candidates for the second $\frac{11}{2}^-$ and $\frac{15}{2}^-$ levels are those at 2706 and 4350 keV in Fig. 1. It was postulated by Gullholmer and Sawa[21] that the levels at 1537, 2233, 2827, and 3592 keV arise from particle-hole excitation of the ground-state configuration. The 4350-keV level further extends this sequence. Theoretical predictions for these states have not been made as yet.

B. ^{54}V

Shell-model predictions for the yrast spectrum of ^{54}V are shown in Fig. 3. These predictions

TABLE VII. γ decay of ^{63}Ni from ^{48}Ca(^{18}O, $3n$) ^{63}Ni.

E_i [a] (keV)	E_f (keV)	E_γ [b] (keV)	Angular distribution [c] I_γ	A_2 (%)	A_4 (%)	τ [d] (ps)
87.13(11) [e]	0	87.13(11) [e]	...	...	...	$2.38(6) \times 10^6$ [e]
1291.79(21)	87	1204.66(18)	55872	19(1)	−11(6)	$4.8(3) \times 10^3$
2183.50(26)	1292	891.70(16)	26076	30(2)	0	5.2(8)
2814.43(29)	2184	630.93(26) [f]	~10000	...	...	0.7 ± 0.3 [g]
	1292	1522.63(20)	15872	13(4)	−15(10)	

[a] Deduced from the γ-ray energies of column 3, including corrections for nuclear recoil. Throughout this table, the figures in parentheses are the uncertainties in the least significant figure. Only levels formed directly in the present studies are included.

[b] Not corrected for nuclear recoil.

[c] Results of fitting the ^{18}O + ^{48}Ca angular distributions with the Legendre polynomial $W(\theta) = I_\gamma[1 + A_2 P_2(\cos\theta) + A_4 P_4(\cos\theta)]$.

[d] Level mean life from the RDM (see Ref. 1) unless otherwise noted.

[e] From Ref. 19.

[f] Observed in coincidence and the RDM only. The energy is derived from the level separation.

[g] From a RDM limit of $\tau < 1$ ps for the 631-keV transition and a DSAM limit of $\tau > 0.4$ ps for the 1523-keV transition.

are due to McGrory (see, e.g., I and II) and utilize the configurational space of Eq. (1) with $m = n = 3$. The monotonic sequence $J, J+1, \ldots$ of our "most probable" level scheme is correctly predicted if we associate the $J^\pi = 3^+$ level with the ground state. However, the tendency, seen in I and II for the McGrory predictions to be too high in excitation energy is here reversed. We note that if the positions of the 469- and 970-keV transitions were interchanged (with a concomitant change in the placement of the 1083- and 1584-keV transitions) the agreement with the predictions would be better. Although the resulting level scheme would not be grossly incompatible with our measurements, it is considered less likely for the experimental reasons discussed in Sec. II B.

C. ^{62}Co

As noted in Sec. II C, if the association of levels between the two schemes of Fig. 4 is correct, then the only spin-parity assignments for the first three levels seen in ^{18}O + ^{48}Ca which are compatible with the (t, ^{3}He) results are 5^+, 5^+, and 6^+, given in order of increasing excitation.

As far as we know there are no published shell-model predictions for ^{62}Co to which we can compare the results of Fig. 4; however, the low-lying yrast spectrum should bear a close resemblance to that of ^{60}Co, for which a rather isolated but closely grouped quartet of $J^\pi = 5^+, 2^+, 3^+, 4^+$ is seen experimentally and predicted theoretically.[2] Assuming such a quartet in ^{62}Co, leads to predictions of 2^+ and 5^+ for the ground state and 22-keV isomeric level, respectively. These assignments are in agreement with those previously conjectured[11] on the basis of the (t, ^{3}He) and ^{62}Co(β)^{62}Ni results.

D. ^{62}Ni

The $1/f_{7/2}$ proton shell is closed at $Z = 28$ and so, to lowest order, the Ni isotopes with $A \geq 57$ have the ground-state configuration

$$(\nu 2p_{3/2}, 1f_{5/2}, 2p_{1/2})^m, \qquad (2)$$

where $m = A - 56$. Koops and Glaudemans[22] have recently published comprehensive shell-model predictions for this configurational space. They utilized a modified surface δ interaction (MSDI) and also a set of one- and two-body matrix elements (ASDI) obtained from a least-squares adjustment of the MSDI matrix elements to experimental binding and excitation energies. In Fig. 8 we compare our energy level scheme for ^{62}Ni to the ASDI results of Koops and Glaudemans. These shell-model predictions appear to account for the yrast and near-yrast levels below 5-MeV excitation. However, this conclusion could well be erroneous. The maximum spin obtainable from the configurational space of (2) with $m = 6$ is 7^+ and there is only one such 7^+ state. Thus, we would contend that the observed levels above 5-MeV excitation arise from excited configurations such as generated by $g_{9/2}$-neutron excitation out of the fp shell or promotion of protons out of the $f_{7/2}$ shell. And, it may be that some of the yrast levels below 5-MeV excitation also arise from such excited configurations. This result for ^{62}Ni is similar to results obtained[2] for ^{59,60}Co where the yrast spectra also extended to higher spins

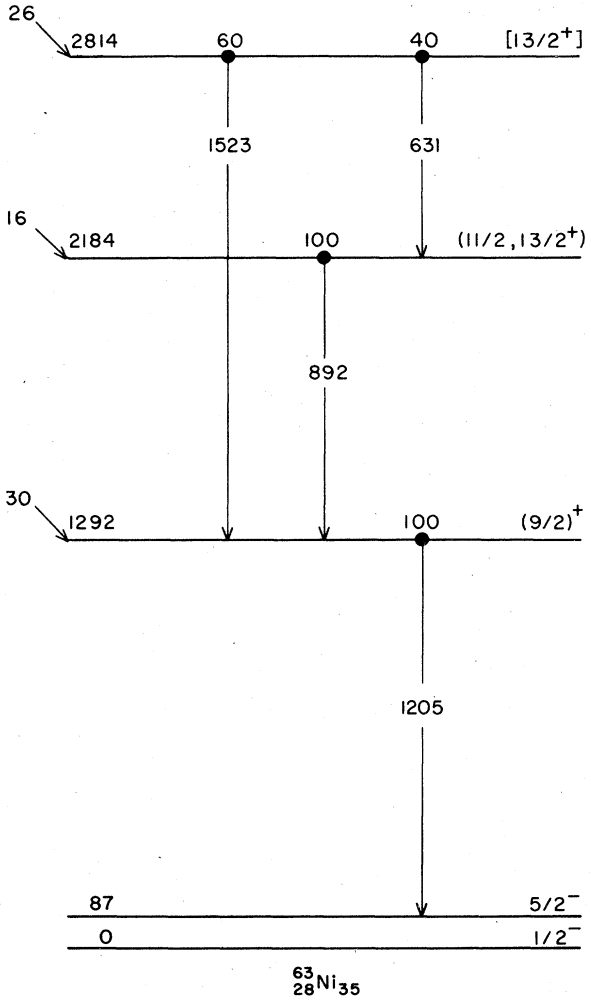

FIG. 7. Level scheme for ^{63}Ni deduced from present studies of the ^{48}Ca(^{18}O, $3n$) ^{63}Ni reaction. Excitation and transition energies are in keV. Relative side-feeding intensities are indicated on the left. Spin-parity assignments enclosed in parentheses are uncertain, those in square brackets are speculative. The assignments for the first three levels are from the compilation (Ref. 19), the upper two are from the present results.

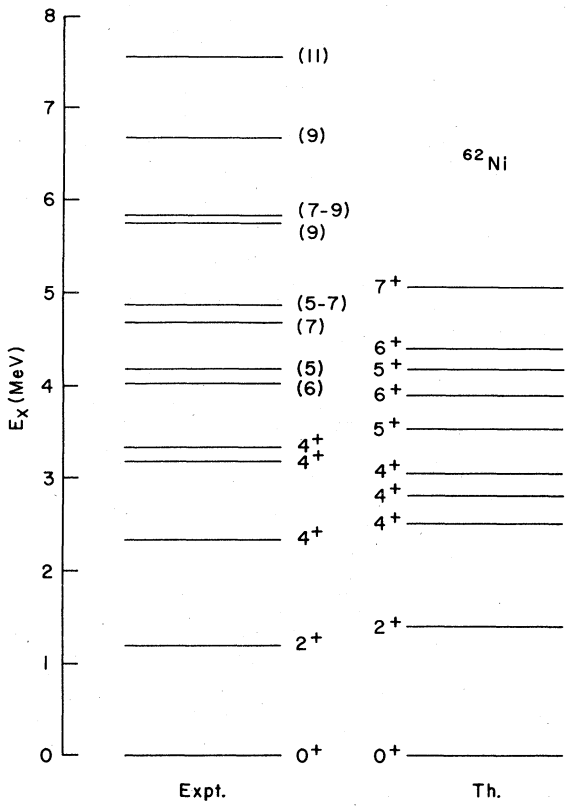

FIG. 8. Comparison of experimental observations and theoretical predictions for yrast states (or near yrast states) for ^{62}Ni. The theoretical spectrum is the ASDI results of Koops and Glaudemans (Ref. 22).

than allowed by the ground-state configuration. Clearly, more definite spin-parity assignments for ^{62}Ni (in particular the parity, π_0, of the 4160-keV level) are needed to help determine the configurations of the ^{62}Ni yrast states.

E. ^{61,63}Ni

Wadsworth et al.[14] compared their results for the odd-parity levels of ^{61}Ni to the predictions of Koops and Glaudemans[22] and found good agreement. We have nothing new to add to this comparison. For ^{63}Ni, the $\frac{1}{2}^-$ ground state and $\frac{5}{2}^-$ 87-keV first-excited state are the only levels with definite odd parity which were observed to be populated in ^{18}O + ^{48}Ca. The next level is, with high probability, $\frac{9}{2}^+$ signaling a $g_{9/2}$ excitation out of the fp shell. Such a situation in which the yrast states of odd nuclei are generated by the coupling of a $g_{9/2}$ orbital to states of the A-1 core has become a familiar feature of the present series of studies of $A = 55$–63 nuclei. In addition to ^{61,63}Ni, as reported herein, such states were observed[2] in ^{59}Fe and also[3] in ^{55}Cr and ^{57}Fe. The most thoroughly investigated of these was ^{57}Fe where the existence of a $\Delta J = 2$ band based on the $\frac{9}{2}^+$ state at 2456 keV was observed up to a probable $\frac{25}{2}^+$ level at 8323 keV. Even parity states interpreted as $g_{9/2}$ orbitals coupled to the lowest 0^+ and 2^+ states of ^{64}Zn and ^{66}Zn have also been observed in ^{65}Zn and ^{67}Zn, respectively.[23]

The available information on yrast and near-yrast states involving $g_{9/2}$ excitations in $A = 54$–67 nuclei is summarized in Fig. 9. As discussed in III, the appearance of the $\Delta J = 2$ bands ($\frac{9}{2}^+$, $\frac{13}{2}^+$,

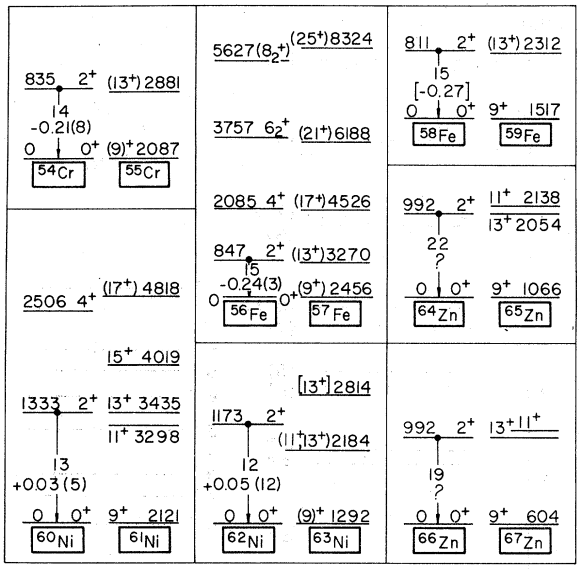

FIG. 9. Comparison of the level spacings between the $J \geq \frac{9}{2}$ even-parity states of ^{55}Cr, ^{57}Fe, ^{59}Fe, ^{61}Ni, ^{65}Zn, and ^{67}Zn with the $\Delta J = 2$ ground-state sequence of the corresponding A-1 nuclei. For the odd-A nuclei $2J$ is shown and only the lowest $\frac{9}{2}^+$ state is included. For the $2^+ \rightarrow 0^+$ transition in the even-A nuclei, the $B(E2)$ in Weisskopf units and the 2^+ quadrupole moment, $Q(2^+)$, in e are indicated by the upper and lower numbers, respectively. For $Q(2^+)$ the uncertainty in the last figure is given in parentheses. The sources for the $B(E2)$ and $Q(2^+)$ values are given in Ref. 24. The spin-parity and excitation energy information given for the odd-A nuclei is from the following sources: ^{55}Cr, ^{57}Fe (Ref. 3); ^{59}Fe (Ref. 2); ^{61}Ni (Ref. 14 and present results); ^{63}Ni (present results and Ref. 15); and ^{65,67}Zn (Ref. 23).

$\frac{17}{2}^+, \ldots$) seen in ^{57}Fe and suggested in ^{55}Cr and ^{59}Fe is characteristic of a decoupled band for which the simplest explanation (among others[3]) is a dominant $Q \cdot Q$ interaction between the odd nucleon and the core. Then if the sign of the product of the quadrupole moments is negative, a decoupled band results with the $J_{\text{core}} + \frac{9}{2}^+$ sequence following closely the energy spacing of the J_{core} sequence and the $J_{\text{core}} + \frac{9}{2}^+ - 1$ levels all lying above the $J_{\text{core}} + \frac{9}{2}^+$ levels. On the other hand, if $Q \cdot Q$ is positive a strongly coupled $\Delta J = 1$ band, $\frac{9}{2}^+, \frac{11}{2}^+, \frac{13}{2}^+, \ldots$, results and, e.g., the $\frac{13}{2}^+ - \frac{9}{2}^+$ spacing is no longer necessarily expected to be close to the 2^+-0^+ spacing of the core. Since the quadrupole moment of the $g_{9/2}$ neutron is negative, we expect $\Delta J = 1, 2$ sequences for A-1 cores with $Q(2^+) > 0, < 0$. In Fig. 9 we include the best information available on the $B(E2)$ and $Q(2^+)$ values for the even-A cores.[24] The available experimental information appears to be in accord with the simple $Q \cdot Q$ prediction. That is, if $Q(2^+)$ is positive (or close to zero) the data are consistent with the supposition that the $\frac{11}{2}^+$ level drops below the $\frac{13}{2}^+$ level and the $\frac{15}{2}^+$ below the $\frac{17}{2}^+$; while for odd $Q(2^+)$ the $J_{\text{core}} + \frac{9}{2}^+$ level would appear to be below the $J_{\text{core}} + \frac{9}{2}^+ - 1$ level for $J_{\text{core}} = 2^+, 4^+, \ldots$, since that situation offers the simplest explanation for the nonappearance of the latter. It must be emphasized that considerably more experimental information [such as on the $Q(2^+)$ values of ^{64,66}Zn and spin-parity assignments for the yrast levels of ^{63}Ni, for instance] is needed before this simple prediction can be adequately tested.

†Research supported by the Division of Basic Energy Sciences, Department of Energy, under Contract No. EY-76-C-02-0016.

*Present address: Physics Department, University of Auckland, Auckland, New Zealand.

[1]A. M. Nathan, J. W. Olness, and E. K. Warburton, Phys. Rev. C 16, 192 (1977).

[2]E. K. Warburton, J. W. Olness, A. M. Nathan, J. J. Kolata, and J. B. McGrory, Phys. Rev. C 16, 1027 (1977).

[3]A. M. Nathan, J. W. Olness, E. K. Warburton, and J. B. McGrory, Phys. Rev. C 17, 1008 (1978).

[4]A. R. Poletti, B. A. Brown, D. B. Fossan, and E. K. Warburton, Phys. Rev. C 10, 2312 (1974); B. A. Brown D. B. Fossan, A. R. Poletti, and E. K. Warburton, Phys. Rev. C 14, 1016 (1976).

[5]R. L. Auble, Nucl. Data Sheets 14, 119 (1975).

[6]R. L. Auble, Nucl. Data Sheets 21, 323 (1977); D. C. Radford and A. R. Poletti (unpublished).

[7]H. Verheul and R. L. Auble, Nucl. Data Sheets 23, 455 (1978).

[8]E. R. Flynn, J. W. Sunier, and F. Ajzenberg-Selove, Phys. Rev. C 15, 879 (1977).

[9]A. M. Nathan, D. E. Alburger, J. W. Olness, and E. K. Warburton, Phys. Rev. C 16, 1566 (1977).

[10]H. Verheul, Nucl. Data Sheets 13, 443 (1974).

[11]F. Ajzenberg-Selove, E. R. Flynn, O. Hansen, J. D. Sherman, N. Stein, and J. W. Sunier, Phys. Rev. C 14, 767 (1976).

[12]D. Bachner, H. Kelleter, B. Schmidt, and W. Seliger, Nucl. Phys. A184, 609 (1972).

[13]P. M. Endt and C. van der Leun, At. Data Nucl. Data Tables 13, 1 (1974).

[14]R. Wadsworth, A. Kogan, P. R. G. Lornie, M. R. Nixon, H. G. Price, and P. J. Twin, J. Phys. G 3, 35 (1977); R. Wadsworth, G. D. Jones, A. Kogan, P. R. G. Lornie, T. Morrison, O. Mustaffa, H. G. Price, D. N. Simister, and P. J. Twin, *ibid.* 3, 833, 1377 (1977).

[15]R. L. Auble, Nucl. Data Sheets 16, 1 (1975).

[16]D. H. Kong-A-Siou and H. Nann, Phys. Rev. C 11, 1681 (1975).

[17]F. Alba, A. Sperduto, and H. A. Enge, private communication reported in Ref. 10 (unpublished).

[18]H. Ohnuma, J. Kasagi, Y. Iritani, N. Kishida, and T. Ogura, Proceedings of the International Conference

on Nuclear Structure, Tokyo, 1977 (unpublished), p. 270.
[19]R. L. Auble, Nucl. Data Sheets 14, 119 (1975).
[20]H. Horie and K. Ogawa, Prog. Theor. Phys. 46, 493 (1971).
[21]W. Gullholmer and Z. P. Sawa, Nucl. Phys. A204, 561 (1973).
[22]J. E. Koops and P. W. M. Glaudemans, Z. Phys. A280, 181 (1977).
[23]See, e.g., P. R. G. Lornie, A. Kogan, G. D. Jones, M. R. Nixon, H. G. Price, R. Wadsworth, and P. J. Twin, J. Phys. G 3, 493 (1977).
[24]Listed here are the sources for the $B(E2)$ and $Q(2^+)$ values of Fig. 8 in the form A, Ref. : 54, Ref. 25: 56. Ref. 26; 58, Ref. 3; 60, Ref. 27; 62, Ref. 26; 64, Ref. 23; 66, Ref. 23. All $Q(2^+)$ were obtained from reorientation measurements except that for ^{58}Fe which is a theoretical prediction.
[25]C. W. Towsley, D. Cline, and R. N. Horoshko, Nucl. Phys. A250, 381 (1975).
[26]A. Christy and O. Häusser, At. Data Nucl. Data Tables 11, 281 (1973).
[27]P. M. S. Lesser, D. Cline, C. Kalbach-Cline, and A. Bahnsen, Nucl. Phys. A223, 563 (1974).